Constructing the Equation of State for Compact Stars

Bachelor thesis

Jan Röder

Contents

List of abbreviations

EOS   equation of state

MRR mass-radius relation

TOV Tolman-Oppenheimer-Volkoff

1   Introduction

To this day, the nature of the equation of state (EOS) for neutron stars is highly debated. Previously discussed EOS have emerged from various topics and models of physics. Each one has different parameters determining its impact on calculations.

For the past years, it has been common to derive an EOS from a theory and then use it to construct a mass-radius relation (MRR). That way, it was somewhat possible to investigate what impact the state of matter in different regions of the star has on a whole sequence. Since science lacks observational information about neutron star radii it has only been possible to put constraints on theories.

This method of constructing MRR has one major limitation: One cannot put an arbitrary number of theories into one EOS. That would result in a problem impossible to solve, even for computers. Therefore, the motivation is to minimize the number of parameters and constraints in the future to find a model that is both solvable and preserves the highest physical relevance.

The approach chosen in this thesis inverts the above process. Instead of using an EOS to calculate masses and radii, the latter now take over the role as input parameters. For compact stars up to a certain mass, the EOS will be assumed to be known well enough. Above that mass a numerical reconstruction will take place, determining the EOS from a variety of MRR. Using the MRR as input leaves us with only the low-density region to impose an EOS in. As explained in 2.3, we have in fact the possibility to model this region sufficiently well. If future measurements grant a decent number of data points on the MRR, an inverse algorithm has the potential to probe the highest densities in the universe. Due to the unique relation of MRR and EOS this would mean a significant contribution to the investigation of high-density phase diagrams of, for example, quark matter. The enormous amount of energy needed to create matter at such densities exceeds everything possible by humanity; therefore a neutron star would be a welcome laboratory.

The first instrument about to attempt neutron star radius measurements is the NICER experiment located at the International Space Station. It will detect x-ray emissions directly from the neutron star's surface and capture the rotational period to determine the radius with a precision of few hundred meters. With that information from multiple neutron stars it could potentially be possible to draw a coarse MRR, with actual data. At that point, EOS reconstruction will likely become a crucial part of neutron star physics.

2 Theoretical background

2.1 Compact stars

At some point in a star's life, it is no longer capable of maintaining nuclear fusion in its core. Hydrogen burning first moves to a shell around the central region, further growing the previously produced helium core up to the point where helium burning ignites. Depending on the star's mass, this process can either repeat until an iron core is formed or stop at some fusion product before that. In the latter case, i.e. for star masses up to $8 \, \mathrm{M_\odot}$, the outer envelopes will escape the core and form a planetary nebula. What remains is a white dwarf, with an upper mass limit given by Chandrasekhar as about $1.4 \, \mathrm{M_\odot}$ [1]. White dwarfs are the first known family of compact objects or -stars. Their interior structure depends on its progenitor star, hence their EOS is not universally defined ([2], p. 91). Their size is of order $10^3 \, \mathrm{km}$, temperatures usually reside in the $10^4 \, \mathrm{K}$ domain but can be one or two orders of magnitude higher ([2], p. 90).
If the fusion processes have produced an iron core, it will be compressed to densities exceeding multiple times the nuclear saturation density when the star turns into a supernova explosion. The type of remnant left behind is called neutron star, and the matter out of which it is formed is always of the same composition and state. Therefore, in contrast to white dwarfs, there is one unique EOS to describe all neutron stars.
Both kinds of compact stars are subject to fast neutrino and photon cooling. After at most a few million years temperatures will have dropped several orders of magnitude below $1 \, \mathrm{MeV}$, so that on the nuclear scale the star can be treated as cold.

2.2 The Tolman-Oppenheimer-Volkoff equation

The equation used for determining the structure of compact stars will here be the TOV equation. To make analytical and numerical calculations easier, the unit system is chosen to be $c = G = 1$, so that every unit is a power of length.
The derivation is based off the assumption that the star matter can be described as a perfect/ideal fluid. Further, the space-time shall not evolve in time, therefore staying spherically symmetric (i.e. it is stationary). In terms of the energy-momentum tensor we are left with:

$$T_{\mu\nu} = (\epsilon + P) \, u_\nu u_\mu - P g_{\mu\nu} \tag{1}$$

Where ϵ is the energy density, P is the pressure and u_μ is the 4-velocity.
Spherical symmetry leads to a certain form of the metric,

$$ds^2 = e^{2\Phi} dt^2 - e^{2\lambda} dr^2 - r^2(d\theta^2 + \sin^2 d\phi^2) \tag{2}$$

containing spherical coordinates r, θ, ϕ and a time-like coordinate t. Equation 2 becomes the line element for a flat space-time if the exponents in the first two coefficients

become zero, from which follows the role of the exponent terms as curvature description in the radial and the time "directions". To be precise, Φ is directly related to gravitational redshift, and λ determines the change of proper length due to curvature. This gives us the stress-energy tensor components:

$$T_{\mu\nu} = diag(\epsilon e^{2\Phi},\ Pe^{2\lambda},\ Pr^2,\ Pr^2 sin^2(\theta)) \tag{3}$$

One now imposes conservation of energy and momentum,

$$\nabla_\nu T^{\mu\nu} = 0 \tag{4}$$

and puts it into the Einstein equations 5 together with the metric, the components of which can be read from 2.

$$R_{\mu\nu} - \frac{1}{2}g_{\mu\nu}R = 8\pi\, T_{\mu\nu} \tag{5}$$

Here, $R_{\mu\nu}$ is the Ricci tensor and R is the Ricci scalar. Both can be calculated from the metric $g_{\mu\nu}$. Before one can get to work to get the actual TOV equations, the metric exponential functions have to be calculated.
One obtains,finally, the full TOV equation:

$$\frac{dP}{dr} = \frac{(\epsilon + P)(m + 4\pi r^3 P)}{2mr - r^2} \tag{6}$$

Together with a second equation for the mass:

$$\frac{dm}{dr} = 4\pi r^2 \epsilon \tag{7}$$

2.3   The equation of state and neutron star structure

Most generally, an EOS determines the relation between a set of quantities that future dynamics of a system can be extrapolated with. Such a set is often referred to as "state variables". Independent of the model applied to a certain type of matter, an EOS takes the form

$$f(p, V, T) = 0$$

with, in this case, pressure p, Volume V and Temperature T. The nature of f (the actual EOS) is then derived from a model (e.g. nuclear or quark) to properly describe the state of matter at hand, be it a fluid, solid or of an exotic type. Here, starting on the outside of a neutron star, states are still in or not far from the range of what can be experimentally observed. Towards the inner regions, exotic states and their impact on the EOS are still subject to investigation. A number of nuclear or fluid EOS have been proposed, each including different aspects like interactions and states of matter, however it remains unclear how exactly a neutron star is built up. While a single EOS for the whole neutron star would be of great interest, one usually determines the EOS

piecewise for each density region separately, imposing a phase transition between the layers. For a brief collection of models, see [3].

The lack of information from direct measurement doesn't particularly improve this situation. However, for the first time, it might be possible to deduce information about the interior of a neutron star through data obtained by the NICER experiment located at ISS.

Generally, a neutron star can be divided into four zones: The inner and outer core, with inner and outer crust above it. These zones have fundamentally different properties. These zones are usually defined through their range of densities. For example, (one finds the original version of this proposal in [3] and [4]), with $[\rho] = \mathrm{g/cm^3}$:

$\rho \leq 10^6$ The *surface* is the outermost region of the star, therefore temperature and magnetic fields can have big impact on the equation of state here. The surface may partly consist of accreted matter of unknown composition, followed by a layer of iron that marks the beginning of the actual neutron star. In this region, the EOS is well approximated by Baym et al. [6] [BPS]. BPS bases calculations on a lattice configuration of nuclei as expected from a lower-density domain. This leads to significant error with respect to the ground state neutron numbers of neutron-rich nuclei further below the surface, as their masses could not be measured with sufficient precision at the time [6] [15].

$10^6 \leq \rho \leq 4.3 \cdot 10^{11}$ Descending into the *outer crust* a Coulomb lattice forms within a relativistic electron gas. Due to charge neutrality, $n_{electrons} = Z \cdot n_{nuclei}$; for the pressure holds $P = P_e + P_L$ [15], where P_L resembles a correction made to account for Coulomb interactions. Upon reaching higher densities, neutronization becomes energetically favorable. In order to determine the nucleus contribution to the energy of one Wigner-Seitz cell in the lattice, BPS subtracting electron rest energies from the atomic masses. The difference between BPS and Haensel et al. [7] [HP] is the model for electron screening effects. BPS used the electron binding energies as such a model, while HP subtracted those as well and imposed electron density uniformities [15] instead.

$4.3 \cdot 10^{11} \leq \rho \leq (2 - 2.4) \cdot 10^{14}$ In the *inner crust* neutron-rich nuclei from a lattice; as the densities increases, neutron drip takes place. Now, there is not only an electron gas, but also a superfluid neutron gas formed by the dripped-out neutrons. A density estimate for the drip to start is performed in [15] starting from

$$E_N(A, Z)/A \simeq E_0 + S_0 \delta^2$$

which is a heavily simplified nuclear mass formula. Terms were neglected until only the symmetry energy S_0 and the energy per nucleon in a symmetric system E_0 are left. $\delta = (N - Z)/A$ is also a remnant from the mass formula. At neutron drip, $\mu_n = E_0 + (2\delta + \delta^2)S_0 = 0$ and therefore $\delta_{\mathrm{ND}} = \sqrt{1 - (E_0/S_0)} - 1$. From the beta

equilibrium condition and an estimate for the electron chemical potential the drip density is about $\rho_{\mathrm{ND}} \simeq 2.2 \cdot 10^{11}\,\mathrm{g/cm^3}$.

As for the EOS, at roughly neutron drip density it is dominated by strong nucleon-nucleon interactions. There are various types of calculations and models for such a many-body system; for example, in [8] Douchin and Haensel use the Skyrme-Lyon [SLy] forces within a liquid drop model for nucleons. Likely, in this bottom region of the crust, nuclei are shaped differently to minimize their surface energy. This was first proposed by Ravenhall et al. 1983 [9], where three basic shapes were used for demonstration. In the domain of the low-density phase, the higher-density phase should form spherical bubbles that turn into rods when descending further into the star. Eventually, both phases should be mixed to equal parts, nuclear matter arranged in planes. From here the process is "reverted"; first, rods of the first phase emerge, turning into bubbles again until only the second, high-density phase is present. This phase transition is often referred to as pasta phase due to the similarities between shapes.

$(2 - 2.4) \cdot 10^{14} \leq \rho \leq \rho_{core}$ The *outer core* or *neutron fluid* does no longer consist of a lattice. Remaining charge neutral, this region is dominated by a neutron superfluid along with a proton superfluid. The charge of the latter is evened out by electrons. In the above discussed liquid drop/SLy model, the crust-core transition appears in the EOS as a (weak) first-order phase transition. The jump in density is in the range 1%. The ground state of nuclear matter can be calculated from the nuclear Hamiltonian [15]. The EOS is determined a little easier; starting from total energy density together with conditions for fixed baryon density and electrical neutrality, Lagrange multipliers give the equilibrium conditions for the chemical potentials. For neutrinos these can be set to zero as they escape the star. Evaluating the first law of thermodynamics at equilibrium leads to the pressure. This calculation can be extended to account for particle fractions varying with density.

$\rho \geq \rho_{core}$ Within the *inner core* lies the biggest mystery. One has no observational information about what processes happen at densities exceeding $10^{15}\,\mathrm{g/cm^3}$. There are various theories about the state of matter in this region; possible are quark core formation or other types of phase transition. As a simple model, $npe\mu$ matter can be extended with a hyperon fraction. This would soften the EOS due to a pressure drop. High-energy neutrons can convert to hyperons, resulting in a lower energy state (which contributes to the pressure) but a higher mass [15].

2.4   General constraints

There are two major conditions for any equation of state to be physically acceptable. For one, it cannot be *ultrabaric*, i.e. $P > \epsilon$. Sometimes this is confused with the superluminal limit even though an EOS might be ultrabaric and still subluminal. A physically relevant EOS cannot be superluminal either, the condition reads $dP/d\epsilon =$

$(v/c_s)^2 < 1$ with effective sound speed c_s. The confusion of the two terms arises because an EOS starts fulfilling both conditions, it will never cross the ultrabaric line. If its slope increases so that $dP/d\epsilon > 1$, the EOS becomes *superluminal*. While a superluminal EOS is widely thought to be acausal, that is not necessarily the case. In general neither Lorentz invariance nor causality explicitly forbid $v > c_s$ [15], but such EOS all have other significant disadvantages leaving them irrelevant.

2.5   Stability, mass-radius relation and third family

The term *stability* is generally used in the context of stability towards perturbations, i.e. radial oscillation modes. This can be read off the mass-radius relation: If the curve reaches a critical point, the slope changes sign and the lowest stable mode switches its stability. Reading from the right, a counter-clockwise change of slope at a critical point leads to instability of a mode. This can be seen in 1. At points A, C and E,
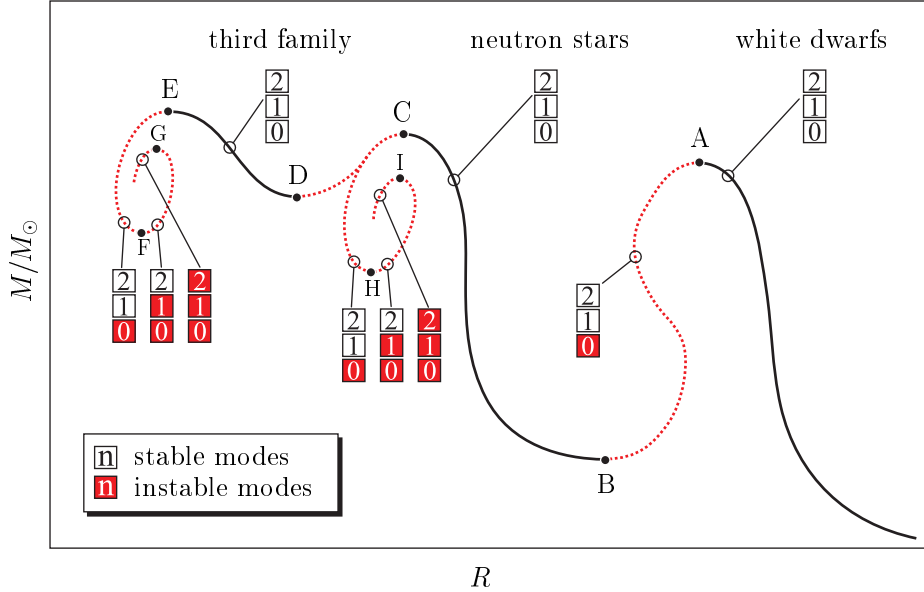

Figure 1: Mass-radius relation with a third stable branch and stability of lowest modes. Taken from [10].

the maximum masses and minimum radii for one family each, the fundamental mode becomes unstable ($n = 0$). n is the number of radial nodes. When a new family starts with its lowest mass, $n = 0$ regains stability. A branch is required to have all modes stable against oscillation to be physically relevant as a family.

A branch usually ends when the EOS becomes sufficiently soft. A phase transition can then lead to a sudden increase in slope, causing the MRR to rise again, to a new branch. For example, a white dwarf is stabilized by the Pauli principle; if it crosses a certain mass limit, it collapses to a neutron star until strong interaction and degeneracy block further compactification. In 1 the neutron star branch hosts mixed phase

cores, i.e. nuclear along with quark matter. Their high-mass twins (more below) do have a mixed phase region, but their core consists of pure quark matter. The interior structure is heavily influenced by the EOS for all three regions, while the hadronic phase EOS is assumed to be known relatively well.

In 1966 Wheeler showed that, if the EOS was smooth, there would only remain a white dwarf and a neutron star branch in the MRR that would contain stable configurations. However, in 2000 Glendenning and Kettner discovered a class of EOS that in contrast to Wheeler's work produced a third stable branch in the MRR [11]. These stars would have the same masses as neutron stars (depending on the exact EOS, this might hold for a certain mass window) but significantly smaller radii. Therefore, these stars are generally referred to as "high mass twins" or "twin stars".

The main arguments against a third family would be instability to oscillations (resulting in explosion oder black hole formation) and distribution of Fermi pressure among more flavors [11]. Most theories resolve around quark core formation and a pasta-like phase transition from hadronic/mixed phase to quark matter analogue to the zone between crust and core.

The first to discover the general possibility of a third family was Gerlach in 1968 [13]; in the process of investigating his theory that some kind of sub-nuclear density interaction may have a significant impact on the EOS and MRR he was also the first to explore an inverse approach to stellar structure calculation. For more on that, see 2.10.

2.6   Yet another compact family?

In 2017 M. Alford and A. Sedrakian were the first to argue what effects a multiple phase QCD diagram would yield for new families of compact stars ([14] and references therein). Up to that point a quark core was always assumed to consist of only one phase.

In order to construct an MRR Alford and Sedrakian put together a piecewise EOS consisting of one for nuclear (hadronic) matter up to saturation density and one for above densities. The latter part is allowed to have two first-order phase transitions, with a constant speed of sound per quark phase. The EOS then looks as follows: From figure 2 a) four of the six parameters determining the EOS can be read off: the transition pressures $P_{1,2}$ as well as $\Delta\varepsilon_{1,2}$, the energy density jumps. The remaining parameters are the phases' sound speeds. Figure 2 b) shows an MRR for four different energy density jump ratios and stiff quark phase EOS. The sound speeds s_1 and s_2 have been set to 0.7 and 1, respectively. For jump ratios above of about 0.15, a fourth branch of compact stars separates from the twin stars located around 12.5 km. White dwarfs are not shown, the very right branch is made of neutron stars. Within a certain ratio range triplet configurations arise: one mass, but three possible radii, depending on the star's composition. This is well visualized in fig. 3. If the phase transitions are sufficiently weakly first order, no instability arises, leaving the MRR with an extended twin star branch. From there, the fourth family emerges, completely vanishing when
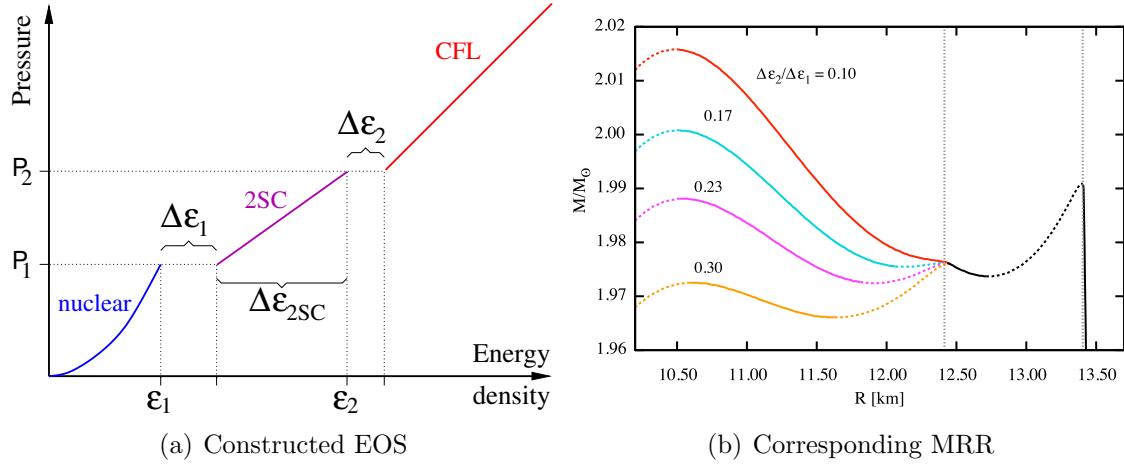
(a) Constructed EOS

(b) Corresponding MRR

Figure 2: (a) Constructed EOS for a second quark matter phase transition. (b) MRR corresponding to stiff two-flavor color superconducting [2CS] and color-flavor-locked [CFL]. Taken from [14].

both transitions are strong enough, making both quark phases unstable.

2.7 Fermi gas equation of state

This EOS will serve as a test case for the reconstruction algorithm (the constant in the polytrope will be set arbitrarily when using it as a first test). For a detailed version of this derivation, see [2].
Here, $p = k$ ($c = 1$) and therefore $E = \sqrt{k^2 + m^2}$. With that, the energy density, pressure and density become:

$$\epsilon = \frac{\gamma}{2\pi^2} \int_0^{k_F} k^2 \sqrt{k^2 + m^2} \, dk \tag{8}$$

$$p = \frac{\gamma}{6\pi^2} \int_0^{k_F} \frac{k^4}{\sqrt{k^2 + m^2}} \, dk \tag{9}$$

$$\rho = \frac{\gamma}{2\pi^2} \int_0^{k_F} k^2 \, dk \tag{10}$$

Setting the chemical potential to $\mu = \sqrt{k_F^2 + m^2}$ (the Fermi energy), the solutions to these integrals read

$$\epsilon = \frac{1}{4\pi^2} \left[\mu k_F \left(\mu^2 - \frac{m^2}{2} \right) - \frac{m^4}{2} \ln \left(\frac{\mu + k_F}{m} \right) \right] \tag{11}$$

$$p = \frac{1}{12\pi^2} \left[\mu k_F \left(\mu^2 - \frac{5m^2}{2} \right) - \frac{3m^4}{2} \ln \left(\frac{\mu + k_F}{m} \right) \right] \tag{12}$$

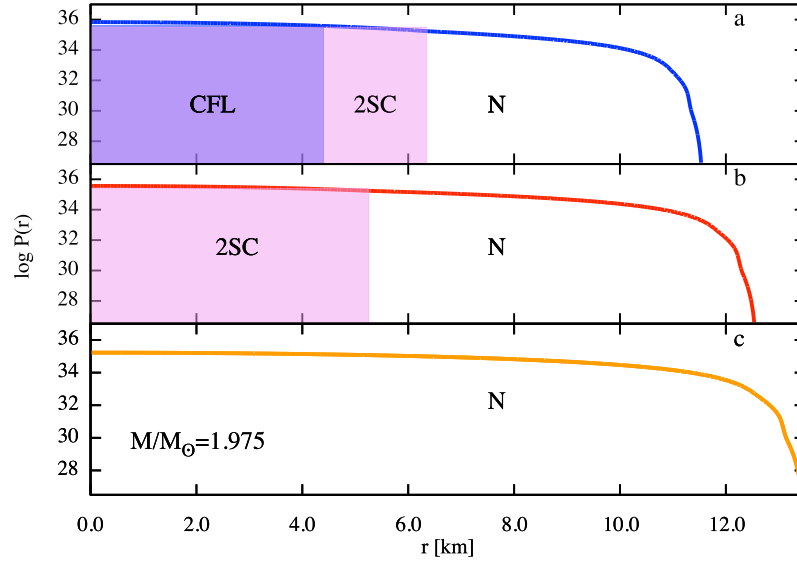$$\rho = \frac{k_F^3}{3\pi^2} \tag{13}$$

Figure 3: States of matter for a triplet configuration. $M = 1.975\,M_\odot$, $\Delta\varepsilon_1/\Delta\varepsilon_2 = 0.23$. Pressure in dyn/cm^2, N stands for Nuclear Phase. Taken from [14].

where $\gamma = 2$, the degeneracy factor for fermions due to spin orientation. The Pauli principle is therefore directly included. Charge neutrality can be imposed, and chemical equilibrium can be obtained as

$$\mu_n = \mu_p + \mu_e \tag{14}$$

with chemical potentials for neutrons, protons and electrons.
Numerically, it is convenient to calculate limits of equations 11 - 13 for the case of high and low densities, i. e. $k_F \gg m$ or $k_F \ll m$. Our test case EOS will resemble very low densities. Expanding 11 in k_F/m one obtains

$$p \sim K \cdot \rho^{5/3} \tag{15}$$

Which is a polytropic type of equation. By absorbing densities into the energy density, one can get

$$p = K \cdot \epsilon^\gamma \tag{16}$$

which is common to use for simple star models, especially white dwarfs.

2.8   Numerical solution

2.8.1   Method

The TOV equations come in the form of a first-order ordinary differential equation system (ODE). In order to obtain sufficient precision, a 4th-order Runge-Kutta algorithm shall be used to solve said ODE. By looking at both equations, our ODE system

is given in the form:

$$\dot{y}(t) = f(y(t), t) \tag{17}$$

where $\dot{y}(t)$ is a two component "vector":

$$\dot{y}(t) = \begin{pmatrix} dP/dr \\ dm/dr \end{pmatrix} \tag{18}$$

$f(y(t), t)$ then contains the right hand side of equations 6 and 7.

Numerically, solving the ODE is achieved by approximation of a step τ in the function variable t (in TOV, this is the radius r) with derivatives of the function that is the ODE solution (y).

$$y(t + \tau) = y(t) + \frac{1}{6}(k_1 + 2k_2 + 2k_3 + k_4) \tag{19}$$

with increments k_i:

$$k_1 = f(y(t), t) \cdot \tau$$
$$k_2 = f(y(t) + k_1/2, t + \tau/2) \cdot \tau$$
$$k_3 = f(y(t) + k_2/2, t + \tau/2) \cdot \tau$$
$$k_4 = f(y(t) + k_3, t + \tau) \cdot \tau$$

All k_i are of course also two component "vectors".

For simpler test versions of the code, it is convenient to reduce the RK4 algorithm to RK1, or Euler's method. Also, the step size does not have to be adaptive. That way, runtime efficiency can be adjusted.

2.8.2 Adaptive step size

In order to maintain a minimum level of precision, the program checks for the change in pressure resulting from one Runge-Kutta step. If said change is too large, the step size τ is varied by a factor and the Runge-Kutta step count is reduced by one. Upon repeating the step, the same check takes place, and if necessary another τ adjustion. If the check is successful, the program will accept the step result and proceed with the next one.

2.8.3 Implementation

In the actual program (written in C), the left hand side of our ODE system is implemented as a two-dimensional array of form y[N][x]. N will be two, for the whole program, as we will not add other equations to the system. The k_i are all one-dimensional arrays; that way x is only reflecting the step count. x will therefore be in range zero up to the number of iteration steps. We set an arbitrary maximum step amount to prevent segmentation faults.

The RK4 algorithm will be implemented so that it can be easily modified any time to another order of Runge-Kutta or even Euler.

2.9   From TOV solver to reconstruction

After implementing the TOV equations together with the integration method, one can now generate an MRR by looping over several p_c and using one EOS only. This MRR will be used for testing the final reconstruction code, which will consist of the TOV solver extended with the reconstruction algorithm explained below.

The main additions will be the split of the pressure range into segments, each requiring their own part of the EOS, as well as a segment determining the "correctness" of calculated mass and radius. The code will work not as "inversely" as was proposed before; the stars will still be integrated from the core towards the surface. However, the reconstruction no longer uses one single EOS.

2.10   The inverse problem

The "standard" problem of stellar structure is an integration of the TOV equations with a given EOS and central pressure, determining the total mass and radius (values of the variables at the surface). The inversion of this "standard" problem was originally brought up by Gerlach in 1968, in a paper investigating the possibility of a third stable family [13]; another well-established method was developed by Lindblom. Both methods shall be recalled here.

Just like any newly published approach to the problem, Gerlach assumes the EOS to be known below a certain density. In order to determine the changes in density and mass for the core region of unknown type for the next configuration, he sets up variations for the TOV equation 6:

$$\frac{d\Delta\rho}{dr} = A(r)\Delta\rho + B\Delta m \tag{20}$$

$$\frac{d\Delta m}{dr} = 4\pi r^2 \Delta\rho \tag{21}$$

Note that Gerlach used ρ instead of ϵ in his equations.

From here he solves the inverse problem in two steps. First, he requires the changes made to a star's surface in terms of radius and mass to be somehow related to changes at the beginning of the core region, here in terms of density and mass. Next, he specifically calculates $\Delta\rho$ and Δm for the core, which are required to smoothly fit to the core surface. Gerlach follows these steps by putting the above equations in matrix form and including an iterative method, as well as setting up proper matching conditions.

Lindblom on the other hand presents an MRR-EOS-pair to be uniquely linked by an abstract map [12]. This gives rise to the possibility of using that map in the other direction, i.e. from MRR to EOS. His "traditional" solution of the inverse problem works as follows:

Instead of integrating the TOV equations from the core towards the surface with initial values $p = p_c$ and $r = 0$, Lindblom uses $M = m(R_{surface}) = m(R)$ and R as starting point to the calculation. Also, the EOS is assumed to be known up to some

pair $\{\epsilon_i, p_i\}$ corresponding to a star $\{M_i, R_i\}$ (as Gerlach did). Looking at the next star, $\{M_{i+1}, R_{i+1}\}$ are set as initial values and integration takes place until $\{\epsilon, p\}$ reach $\{\epsilon_i, p_i\}$. At this point, a core $\{m_{i+1}, r_{i+1}\}$ is left to be integrated. By representing the TOV equations for this small region as a power series, and inverting that, one can obtain $\{\epsilon_{i+1}, p_{i+1}\}$ as a function of previously calculated quantities. This algorithm is repeated for the rest of the MRR, using an interpolation method to link $\{\epsilon_{i+1}, p_{i+1}\}$ to the known EOS.

Here, a different and more simplistic approach to this problem is developed. This new method does not require the star to be integrated from crust to core, but will merely be a modification of the standard problem. This leads to a kind of "trial and error" type of solution, as section 3 will explain more detailed.

3 Reconstruction method

3.1 General goal

The goal is to reconstruct the EOS with as few biasing and imposing of mathematical form as possible. Therefore, the only pre-determined input is an EOS corresponding to a given mass in the MRR (Fig. 4). From there, the EOS can be constructed without further constraint. Here, a straight line is added to the end of the EOS, that is, in the high density region (Fig. 5 b). The ODE solver starts at a point near the end of the given EOS and will calculate a mass with the (now small) piece of straight line and the EOS. If the mass does not fit the corresponding one in the MRR that was read in previously, the starting point on the line will be shifted to a higher pressure by a small step. At some very high pressure, a cut-off can be applied due to un-physical energy densities. If the starting point reaches the cut-off and the correct mass was not found, the slope of the line is varied. The latter also happens when the radius that corresponds to the calculated mass does not fit the one corresponding to the radius in the file. in Fig. 5 c) the slope and end point of the green line have been successfully varied and the next mass and radius are reconstructed using the variation of the red line. The green line is now a part of the given EOS. This process will be repeated until the end of the MRR file.

3.2 Pressure intervals

For the first mass in the file that is supposed to be reconstructed, the code will use the given EOS over the complete pressure interval p_c to 0. That way, the first mass can be reproduced exactly in a test case. p_c will be the last pressure value of the given EOS interval. From there, lines will be added to that end point; in the program, a flag labelled "one" will be set to false after the first mass was calculated.

From this point on it is important to determine which EOS will be used for what pressure interval inside the star. The second mass to be calculated will use the given EOS and one single line after it; masses number three and above then also need a line,
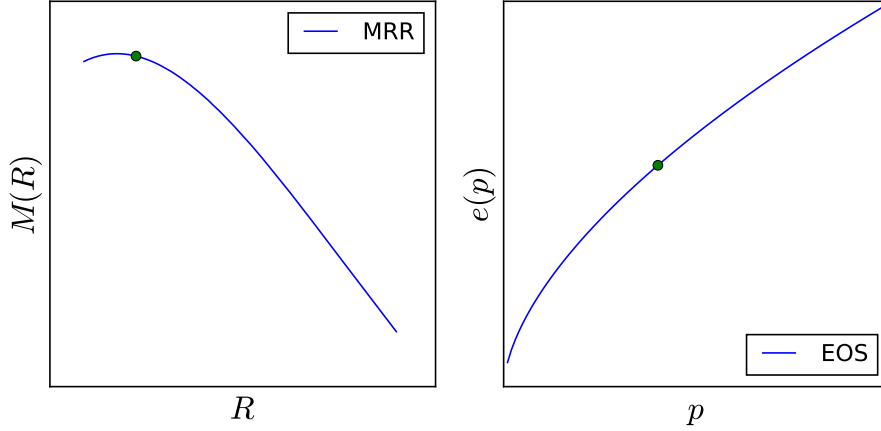
Figure 4: corresponding points in MRR and EOS. Point in EOS resembles values in the center of the star.

but before finishing with the given EOS the previously determined lines are supposed to fill in the rest of the pressure range.

The line currently subject to variation will start at the central pressure (p_c) and will end at the last pressure a star was reconstructed for. This is resembled by the end point of the last previous line (or in the special case, the last pressure of the given EOS). The last given EOS pressure is saved in the very beginning as p_{init}, marking the point from which the given EOS will finish up the mass calculation.

3.3   Linear interpolation

Four parameters are needed to calculate one line equation (two points in a two-dimensional plane). In the code, every EOS point consists of a pressure and an energy density value. The parameters needed for one line are stored in an array α:

$$(\alpha_0,\ \alpha_1,\ \alpha_2,\ \alpha_3) = (p_1,\ \varepsilon_1,\ p_2,\ \varepsilon_2)$$

Inserting this array into $y = mx + b$ or rather $\varepsilon = mp + b$, the line equation looks as follows:

$$\varepsilon(p) = (p - \alpha_1)\frac{\alpha_3 - \alpha_1}{\alpha_2 - \alpha_0} + \alpha_0 \tag{22}$$

where $m = \Delta\varepsilon/\Delta p$ and b is the y axis point. While one line is being varied, α_0 and α_1 stay fixed as they are the last line's end point. Calculating the mass, α_2 is varied at fixed α_3. If the corresponding radius does not fit, α_3 is shifted through a slope change. If mass and radius have been reconstructed with sufficient precision, the α array is extended by two in order to fit in the next end point to be varied. The EOS function always checks which interval the current pressure lies in to determine the α for further calculation. The array will be extended to index values high above three; here, zero to three were chosen. In the actual program, (α_0, α_1) resembles the known
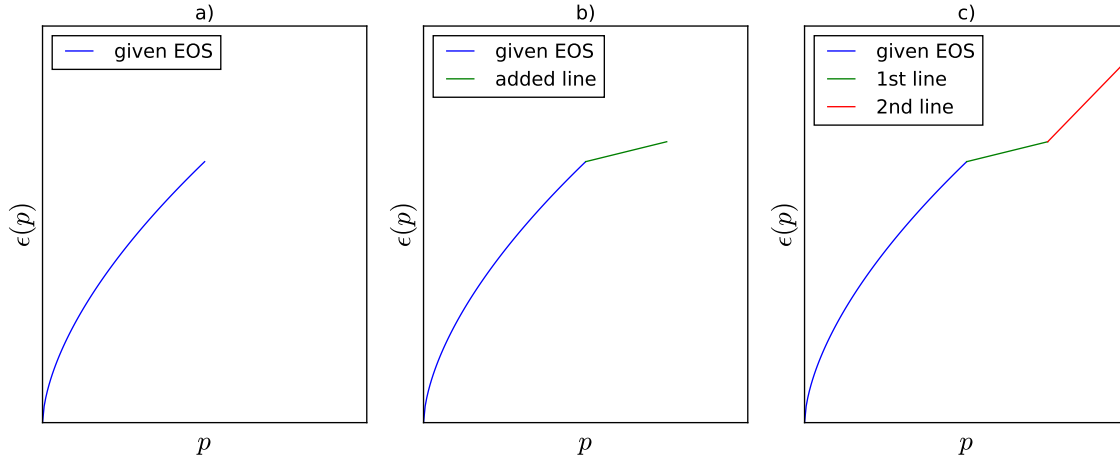
13

Figure 5: a) Given polytropic equation of state, b) added a constructed straight line, c) Successfully varied green line, red line for next mass

EOS region's end. In order to generalize equation 22, in index i is introduced and initialized with alpha.size()-2. In the above special case, alpha.size() (C function) would equal to four. The subscripts in 22 are now rewritten with i:

$$\varepsilon(p) = (p - \alpha_{i-1}) \frac{\alpha_{i+1} - \alpha_{i-1}}{\alpha_i - \alpha_{i-2}} + \alpha_{i-2} \tag{23}$$

That way, the array can be more easily accessed an used by the code even with continuous extension.

Centering the whole reconstruction around the α array also immediately makes external EOS input possible. An EOS table read in by the code along with an MRR would be stored in α and used for the calculation with either the same linear function as the rest, or with another interpolation method. Note that the external table would need the energy density density in one column (many EOS use the matter or baryon density instead).

3.4   Indirect radius check

Upon finishing the calculation for a star, the code is to check mass and radius. This can either be done by directly comparing the calculated values with the input (in the following, direct method) or by choosing an indirect way of doing so. The direct method can be described as a search for the root of a function f_{dir}:

$$f_{\text{dir}} = R_{\text{calc}} - R_{\text{want}}$$

While the direct method somewhat works in the low-density region, it quickly starts suffering from big slope jumps for the reconstructed lines. Some MRR points are found corresponding to values above the wanted EOS curve, continuing with only

very slight changes in slope until points below the EOS are used. From there, a slope jump pushes the next point above the curve again. The jumps get bigger exponentially up to a point where the code cannot push above the EOS again; from here, none of the produced values are of use.

A way to work around these jumps is by choosing an indirect method function f_{ind}:

$$f_{\text{ind}} = (R_{\text{calc}} - R_{\text{want}})^2 + \lambda \cdot (\xi_{\text{curr}} - \xi_{\text{prev}})^2$$

Instead of trying to find the roots of f_{dir}, the code is supposed to find extrema of f_{ind}. The functions are related as

$$f_{\text{ind}} \sim \int f_{\text{dir}}$$

λ is an "importance parameter". In order to avoid big jumps in the slope ξ_{curr} with respect to ξ_{prev}, λ is set to some value. That way, ξ_{curr} will not deviate more from ξ_{prev} than λ allows. Before the variation of a slope, a star is calculated once with the current slope and with a higher and lower one, respectively. The slope variation direction is then determined by the behaviour of f_{ind}. After the first reconstruction λ is set to a value above zero while initially using $\lambda = 0$ as there is no slope from before to use. There is no way of determining a "perfect" λ other than trial and error; the parameter remains rather arbitrary and therefore has to be set out of numerical reasons.

Some time in the future, the program should be capable of modelling first-order phase transitions in the EOS. Such a transition requires a jump in the slope and discontinuities in the EOS. It is obvious that the indirect method is biased towards smooth EOS without any unusual progression − ruling out the possibility to model a phase transition from the beginning. That can be dealt with by tracking extremal points in the MRR while reading it in as input. When the reconstruction part of the code reaches the first mass behind a maximum, the algorithm is changed from f_{ind} to f_{dir} by setting $\lambda = 0$. ξ_{curr} may now freely deviate from ξ_{prev} to find the EOS points during and after the transition.

Setting $\lambda = 0$ of course bears the risk "finding" wrong points easily as there is less control over how the calculation deals with the extra degree of freedom. Especially, the minimal radius changes have to be taken into account: often, the slope may change significantly, while leaving the radius either unchanged or changing it in the order of 10^{-5} km.

3.5   Test case

The first code test will take place with a simple polytropic EOS such as

$$\epsilon(p) = \left(\frac{p}{10} \right)^{3/5}$$

Using the TOV solver, an MRR is generated. For this simple case, RK4 was reduced to Euler's method and the step size is not adaptive. The MRR seen in Fig. 6 will be
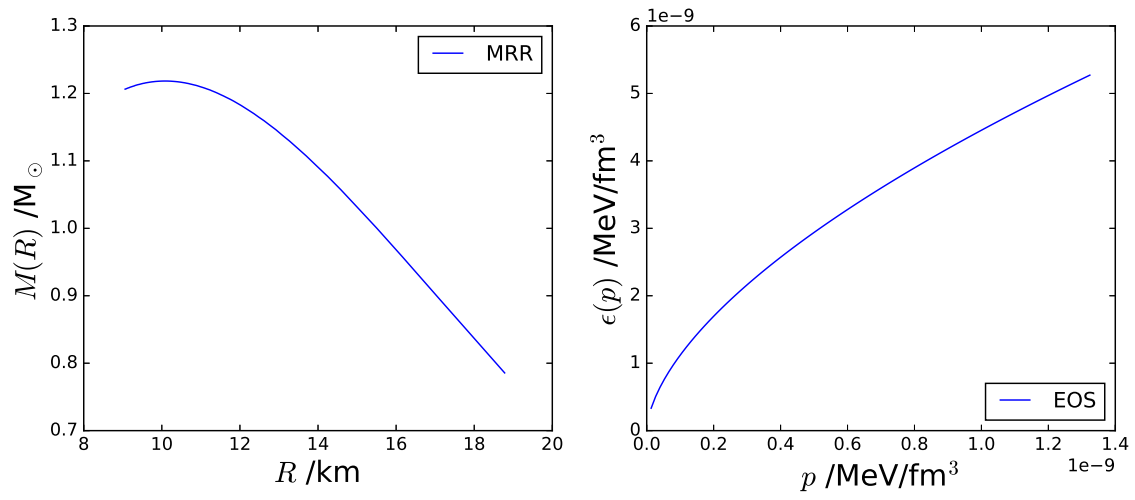
Figure 6: Test case

Figure 7: Reconstruction test

the first one to be reconstructed. The curves both consist of 100 data points which will be read in by the reconstruction code. The result can be seen in 7.

4   Results

4.1   Issues

References

[1] Mazzali, P. A., Röpke, F. K., Benetti, S., & Hillebrandt, W. 2007, Science, **315**, 825

[2] Glendenning, N. K., Compact Stars: Nuclear Physics, Particle Physics, and General Relativity, Springer-Verlag New York, 2000, 1997

[3] Pandharipande, V. R., Pines, D., & Smith, R. A. 1976, Astrophys. J., **208**, 550

[4] Shapiro, S. L., & Teukolsky, S. A. 1983, Research supported by the National Science Foundation. New York, Wiley-Interscience, 1983, **663**, p. 252

[5] Harrison, B. K., Thorne, K. S., Wakano, M., & Wheeler, J. A. 1965, Gravitation Theory and Gravitational Collapse, Chicago: University of Chicago Press, 1965

[6] Baym, G., Pethick, C., & Sutherland, P. 1971, Astrophys. J., **170**, 299

[7] Haensel, P., & Pichon, B. 1994, A&A, **283**, 313

[8] Douchin, F., & Haensel, P. 2001, A&A, **380**, 151

[9] Ravenhall, D. G., Pethick, C. J., & Wilson, J. R. 1983, Physical Review Letters, **50**, 2066

[10] Schertler, K., Greiner, C., Schaffner-Bielich, J., & Thoma2, M. H. 2000, Nuclear Physics A, **677**, 463

[11] Glendenning, N. K., & Kettner, C. 2000, A&A, 353, L9

[12] Lindblom, L. 1992, Astrophys. J., **398**, 569

[13] Gerlach, U. H. 1968, Physical Review, **172**, 1325

[14] Alford, M., & Sedrakian, A. 2017, Physical Review Letters, **119**, 161104

[15] Haensel, P., Potekhin, A. Y., & Yakovlev, D. G. 2007, Astrophysics and Space Science Library, 326, Haensel